COVID-19 severity stratification using quantitative computed tomography analysis

Kantitatif bilgisayarlı tomografi analizi kullanılarak COVID-19 şiddet derecelendirilmesi

Akın Çinkooğlu[1] Habib Ahmad Esmat[1] Mustafa Bozdağ[2] Selen Bayraktaroğlu[1]

Naim Ceylan[1] Mehmet Soylu[3] Recep Savaş[1]

[1] Ege University Faculty of Medicine, Department of Radiology, Izmir, Türkiye

[2] Tepecik Training and Research Hospital, Department of Radiology, Izmir, Türkiye

[3] Ege University Faculty of Medicine, Department of Medical Microbiology, Izmir, Türkiye

ABSTRACT

Aim: This study aimed to examine the utility of computer-assisted quantitative assessment of chest computed tomography (CT) images in the stratification of Coronavirus Disease 2019 (COVID-19) severity.

Materials and Methods: This study was designed as a retrospective, single-center study and included a total of 142 RT-PCR-confirmed COVID-19 patients. CT findings were visually evaluated and noted for their morphology and distribution characteristics. Visual semi-quantitative score (VSS) and computer-aided quantitative score (CQS) were calculated. The utility of the approach was assessed based on its ability to predict the patients who would require intensive care.

Results: The presence of underlying fibrosis, air bubble sign, and co-occurrence of central and peripheral lung area involvement were the CT findings that were significantly more commonly encountered in patients with intensive care requirements during the follow-up period. We found a significant positive correlation between total VSS and CQS (p<0.001). Total CQSs were significantly higher in ICU patients (n=19) than non-ICU patients (n=123) (p<0.001).

Conclusion: Computer-aided quantitative assessment appears to be a valuable tool for radiologists to assess the severity of COVID-19 pneumonia.

Keywords: COVID-19, thorax, tomography.

ÖZ

Amaç: *Bu çalışma, Koronavirüs Hastalığı 2019 (COVID-19) şiddetinin sınıflandırılmasında göğüs bilgisayarlı tomografi (BT) görüntülerinin bilgisayar destekli kantitatif değerlendirmesinin faydasını incelemeyi amaçlamıştır.*

Araçlar ve Yöntem: *142 RT-PCR COVID-19 hastasını içeren retrospektif, tek-merkezli bir çalışma tasarladık. Morfoloji ve dağılım özelliklerine göre BT bulgularının görsel değerlendirmesi not edildi. Görsel yarı kantitatif skor (GKS) ve bilgisayar destekli kantitatif skor (BKS) hesaplandı. Yaklaşımın faydası, yoğun bakıma ihtiyaç duyacak hastaları tahmin etme yeteneğine göre değerlendirildi.*

Bulgular: *Altta yatan fibrozis varlığı, hava kabarcığı bulgusu, santral ve periferik akciğer alanı tutulumu birlikteliği takip döneminde yoğun bakıma ihtiyacı olan hastaların BT görüntülerinde anlamlı olarak daha yüksek oranda görülen bulgulardı. Total GKS'lar ve BKS'lar arasında anlamlı pozitif korelasyon saptadık (p<0.001). YBÜ hastalarının (s=19) toplam BKS'ları, YBÜ'de olmayan hastalardan (s=123) anlamlı derecede yüksek saptandı. (p<0.001).*

Corresponding author: Akın Çinkooğlu
Ege University Faculty of Medicine, Department of Radiology,
Izmir, Türkiye
E-mail: *acinko@gmail.com*

Sonuç: *Bilgisayar destekli kantitatif değerlendirme, radyologların COVID-19 pnömonisinin şiddetini değerlendirmeleri için değerli bir araç gibi görünmektedir.*

Anahtar Sözcükler: *COVID-19, toraks, tomografi.*

INTRODUCTION

Chest computed tomography (CT) is a valuable tool in managing COVID-19 pneumonia. Recognition of typical CT findings allows early detection and isolation of patients with false-negative initial reverse transcriptase-polymerase chain reaction (RT-PCR) results (1, 2). In addition, temporal changes in the density and distribution pattern of parenchymal opacities may be helpful in estimating the disease stage (3, 4). As a consequence of the rapid increase in the number of CT examinations performed and the need for accurate assessment and staging of COVID-19 pneumonia, an effective and accurate assessment technique is needed.

Quantification of radiological data with scoring systems is critical for standardizing results. There are several visual scoring systems designed for this purpose. Nevertheless, the importance of inter-observer consistency and producing objective and reproducible results in devising a standard scoring algorithm should always be considered (5). Objective assessment using computer-assisted quantification may be an appropriate approach to stratify patients according to the severity of COVID-19 (6).

In our study, we aim to evaluate the value of quantitative CT evaluations using computer-based tools in determining disease severity in patients with COVID-19 pneumonia and compare this approach's effectiveness with that of visual analysis methods to describe the most appropriate approach serving this purpose.

MATERIALS and METHODS

Patients

This study was approved by the Ethics Committee of our institution (Approval Number: 20-12.1T/42). We retrospectively analyzed the high-resolution CT (HRCT) images of 276 consecutive RT-PCR-positive COVID-19 patients who applied to our hospital between 04.03.2020 and 19.04.2020. Patients over 18 years of age with positive CT findings consistent with pneumonia were included in the study. Patients with inadequate radiological image quality that impaired visual and computer-assisted scoring were excluded. A total of 142 patients (73 men and 69 women, age range 19-95, mean age 53.50 ± 15.92 years) who met the criteria were included.

CT Image Acquisition

Computed tomography images covering the chest inlet to the diaphragm were acquired in high-resolution imaging protocol using a 160-slice-CT scanner (Aquilion Prime, Toshiba Medical Systems, Tokyo, Japan). The scanning parameters were: 80 x 0.5 mm collimation, 120 kVp, automated dose reduction, and reconstruction with a sharp algorithm at 0.5 mm slice thickness. Images in the axial plane were acquired at shallow inspiration during a single breath-hold without contrast media. Images were sent to the workstation (Gemstone Spectral Imaging Imager Software, GE Healthcare) for visual evaluation of CT findings and calculation of visual semi-quantitative score (VSS) and computer-assisted quantitative score (CQS) using Thoracic VCAR (v.13). Images were viewed using optimized window settings for lung parenchyma assessment.

CT Visual Evaluation and Calculation of VSS and CQS

Visual evaluations of computed tomography images were analyzed by two radiology specialists, one with 16 years and the other with 6 years of experience in thoracic radiology. These evaluators were blind to the results of the computer-assisted assessment of the patients. The distribution pattern of the lesions (transverse, craniocaudal, and anterior-posterior distributions, as well as focality and laterality) and their morphological features (ground-glass opacity -GGO-, GGO with consolidation, crazy-paving pattern, air bubble sign, pure consolidation, halo sign, reverse halo sign, air-bronchogram, vascular enlargement, bronchiectasis, subpleural line) were noted. VSSs were then calculated according to the method described by Chung and colleagues (7). Briefly; for each of the five lobes, the involved area within each lobe was scored visually as 0 (0% or no lung involvement), 1 (1%–25% of the lobe volume involved), 2 (26%–50% involved), 3 (51%–75% involved), or 4 (76%–100% involved). Cases in which the primary evaluators disagreed were evaluated by a third experienced thoracic radiologist (with 25 years of experience), and the final decision was reached by consensus. Computer-assisted evaluation to

obtain the CQS included total lung segmentation, segmentation of the five lobes, segmentation of pulmonary vasculature and airways, calculation of total lung volume and volumes of each lobe separately, and determination of the percentage of the involved volumes within the entire lung and each lobe. The interval between -950 HU and -700 HU was used to define a normal lung in software segmentation (Figure-1).
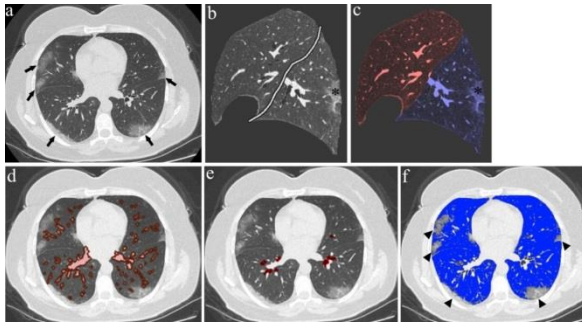
Figure-1. Steps of computer-aided evaluation (a-f). Axial CT image (a) shows bilateral, peripherally distributed ground-glass opacities (arrows), a typical CT finding in COVID-19 pneumonia. After obtaining fully automated lung parenchyma segmentation, manual fissure tracing was performed on the sagittal reformatted images of extracted lung parenchyma to obtain lobar segmentation (b). Segmented left upper lobe (red color), left lower lobe (blue color), and peripheral ground-glass opacities (star) are seen in the colored lung image (c). Segmentation of pulmonary vascular structures (d) and segmentation of airways (e) are demonstrated on axial images. Normally-aerated lung parenchyma (blue color) and peripheral parenchymal ground-glass opacities (arrowheads) are shown on the axial image (f), demonstrating the parenchymal analysis steps.

Statistical Analysis

Statistical analysis was performed using SPSS statistical package (IBM, version.25.0, Chicago, USA). Normally distributed continuous data were expressed as mean ± standard deviation. Non-normally distributed continuous data were expressed as median values. Mann-Whitney U test and the two-sample t-test were performed for the comparison of independent groups. For correlation analysis, Spearman correlation analysis was done. Receiver Operator Characteristics Curve (ROC) analysis was done

to obtain the cut-off value. A p-value less than 0.05 was noted as statistically significant.

RESULTS

Evaluation of COVID-19 Pneumonia CT Findings

We evaluated CT images of 142 COVID-19 patients (73 men and 69 women; age range: 19-95 years; mean age: 53.50 ± 15.92 years) confirmed by RT-PCR and chest CT. Of our patients, 123 remained stable throughout their hospital stay and were followed up in a non-critical hospital ward (non-ICU patients), whereas 19 were transferred to the intensive care unit (ICU) (ICU patients). We analyzed lesions' location, distribution, and morphology based on visual interpretation of CT images to identify possible distinguishing differences between ICU and non-ICU patients (Table-1). All 19 ICU patients had multifocal lesions. Bilateral lung involvement was detected in 18 cases (94.7%), and lesions did not show a zonal predilection in most of these patients (63.2%). Lesions in non-ICU patients showed bilateral (87.0%) and multifocal (88.7%) patterns, similar to ICU patients. However, the lesions in this group of patients showed a predilection for the lower zones of the lung. There was a significant difference in the transverse distribution pattern of the lesions between the two groups (p = 0.008). Lesions showed both central and peripheral distribution in 78.9% of ICU patients (Figure-2a); however, of the non-ICU patients, only 40.7% had such a distribution pattern, and 58.5% showed only peripherally distributed lesions. As for morphological assessment, pure GGO (patchy and/or nodular) was the most common (81%) pattern. This was followed by GGO with consolidation (30.3%), crazy-paving pattern (23.2%), and GGO with pure consolidation (15.5%). This order of incidence was similar in both groups. Halo sign, reverse halo sign, air-bronchogram, subpleural line, vascular enlargement, air bubble sign, and bronchiectasis were other CT findings seen at different rates in both ICU and non-ICU patients. Of these CT findings, only the air bubble sign (i.e., small air-containing spaces within the lung opacity) was significantly higher in ICU patients (26.3%) than in the non-ICU group (8.9%) (Figure-2b). Underlying fibrosis was another distinguishing factor that was significantly higher in the ICU group (21.1%) than in the non-ICU cases (3.3%).

Table-1. Patient Characteristics and comparison of visual CT imaging findings of COVID-19 pneumonia based on intensive care necessity (n=142) Number of cases & percentages.

	ICU (severe) patients (n=19)		Non-ICU (non-severe) patients (n=123)		Total n = 142	%	P value [a]
Age (mean ± SD)	63.74 ± 18.42		49.98 ± 14.75				0.003[*]
Gender							
Male	12	16.4	61	83.6	73		0.271
Female	7	10.1	62	89.9	69		
Laterality							
Unilateral	1	5.3	16	13	17	12	0.470
Bilateral	18	94.7	107	87	125	88	
Focality							
Unifocal	0	0	14	11.3	14	9.8	0.301
Multifocal	19	100	109	88.7	128	90.2	
Transverse distribution							
Central	0	0	1	0.8	1	0.7	0,008[*]
Peripheral	4	21.1	72	58.5	76	53.5	
Diffuse	15	78.9	50	40.7	65	45.8	
Craniocaudal distribution							
Upper lung predominant	1	5.3	11	8.9	12	8.5	0.104
Lower lung predominant	6	31.6	66	53.7	72	50.7	
Diffuse	12	63.2	46	37.4	58	40.8	
Anteroposterior distribution							
Anterior	1	5.3	10	8.1	11	7.7	0.119
Posterior	5	26.3	60	48.8	65	45.8	
Diffuse	13	68.4	53	43.1	66	46.5	
Density							
Pure GGO	15	78.9	100	81.3	115	81	0.760
GGO with consolidation	6	31.6	37	30.1	43	30.3	0.895
Crazy-paving pattern	5	26.3	28	22.8	33	23.2	0.772
Pure consolidation	6	31.6	16	13	22	15.5	0.080
Other CT findings							
Halo sign	1	5.3	15	12.2	16	11.3	0.696
Reverse halo sign	3	15.8	19	15.4	22	15.5	1.000
Air-bronchogram	6	31.6	26	21.1	32	22.5	0.376
Air bubble sign	5	26.3	11	8.9	16	11.3	0.042[*]
Subpleural line	3	15.8	38	30.9	41	28.9	0.176
Vascular enlargement	7	36.8	43	35	50	35.2	0.873
Bronchiectasis	7	36.8	23	18.7	30	21.1	0.126
Underlying fibrosis	4	21.1	4	3.3	8	5.6	0.012[*]

[a] P-values calculated by Chi-square tests, p<0.05 shows statistical significance ([*]).

CT, Computed tomography; GGO, ground glass opacity; ICU, Intensive care unit.

Table-2. Comparison of the patient groups (ICU vs non-ICU) based on the CQSs (n=142).

	ICU (severe) n=19	Non –ICU (non-severe) n=123	
	median	median	P value [a]
RLL - CQS	41.97	14.84	<0.001[*]
RML - CQS	22.00	9.38	<0.001[*]
RUL - CQS	28.51	10.88	<0.001[*]
RT - CQS	29.99	12.58	<0.001[*]
LLL -CQS	28.24	15.68	<0.001[*]
LUL - CQS	18.46	10.26	<0.001[*]
LT - CQS	23.83	13.14	<0.001[*]
TOTAL - CQS	27.04	12.86	<0.001[*]

[a]P-values calculated by Mann-Whitney U test, p<0.05 shows statistical significance ([*]).

Abbreviations: CQS, Computer-aided quantitative score; ICU, Intensive care unit; LLL, Left lower lobe; LUL, Left upper lobe; LT, Left total; RLL, Right lower lobe; RML, Right middle lobe; RUL, Right upper lobe; RT, Right total.

Table-3. Correlations of lobar and total VSSs and CQSs; p values & correlation coefficients [a] (rs) (n=142).

|	RLL-VSS	RML-VSS	RUL-VSS	RT-VSS	LLL-VSS	LUL-VSS	LT-VSS	TOTAL-VSS
RLL CQS	- rs=0.568 p<0.001[*]							
RML CQS	-	rs=0.599 p<0.001[*]						
RUL CQS	-		rs=0.600 p<0.001[*]					
RT- CQS				rs=0.643 p<0.001[*]				
LLL CQS	-				rs=0.540 p<0.001[*]			
LUL CQS	-					rs=0.548 p<0.001[*]		
LT - CQS							rs=0.643 p<0.001[*]	
TOTAL CQS	-							rs=0.648 p<0.001[*]

[a]Spearman correlation coefficient (rs); 0.3 – 0.5 moderate to low; > 0.7 strong positive correlations, p<0.05 shows statistical significance ([*]).

VSS,Visual semi-quantitative score; CQS, Computer-aided quantitative score; LLL, Left lower lobe; LUL, Left upper lobe; LT, Left total; RLL, Right lower lobe; RML, Right middle lobe; RUL, Right upper lobe; RT, Right total.

VSS and CQS evaluation

Visual semi-quantitative scores and CQSs were calculated for the five lung lobes separately, and these were summed to obtain the total scores. The most affected lobe was the right lower lobe, and only 17 patients (12%) had no lesions in the right lower lobe (VSS-grade 0). Computed tomography images of 11 patients showed an involvement rate of over 75% (grade 4). The left upper lobe was the least affected, and only six patients (4.2%) had more than 50% involvement (VSS-grade 3-4). Likewise, when the involvement was investigated according to CQS measurements, the right lower lobe showed the highest scores, and the lung parenchyma involvement rate was more than 50% in 12 patients (8.4%). The CQSs were significantly higher in the ICU group, indicating that patients requiring intensive care during the follow-up showed more extensive lung involvement (Table-2). Total CQSs of ICU patients (n = 19, median = 27.04) were significantly higher (p < 0.001) than non-ICU patients (n = 123, median = 12.86). A significant positive correlation was found between total VSSs and CQSs (rs = 0.648, p < 0.001) (Figure-3). VSS and CQS values for each lung lobe were also positively correlated with each other (p < 0.001) (Table-3). The CQS cut-off value in predicting patients that required intensive care during the follow-up period was calculated as 13.51 (AUC = 0.804, 95% CI = 0.693-0.914). This cut-off had 85% sensitivity and 60% specificity (Figure-4).
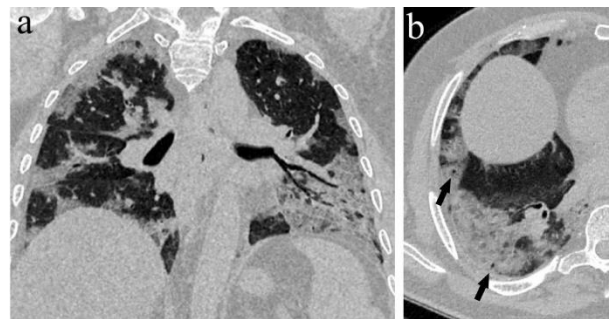
Figure-2. Distinctive CT features of intensive care patients (a-b) Coronal reformatted image (a) shows the crazy-paving pattern and consolidations with both central and peripheral distribution. Axial CT image (b) shows small air-containing cavities consistent with the air bubble sign (arrows). This patient had a total VSS of 19 and a total CQS of 52.5 and required intensive care during the follow-up period.
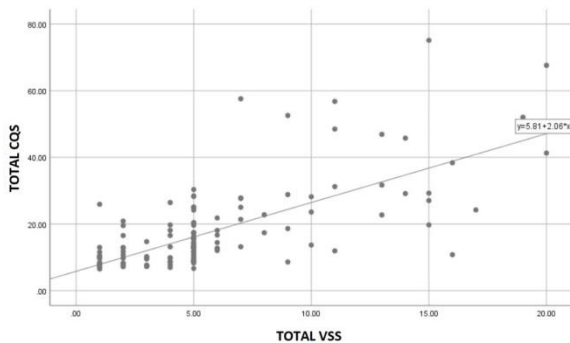
Figure-3. Scatter plot graph of the correlation between total CQSs and total VSSs. The graph shows the significant positive correlation between total CQSs and total VSSs (rs=0.648, p<0.001). VSS, Visual semi-quantitative score; CQS, Computer-aided quantitative score.
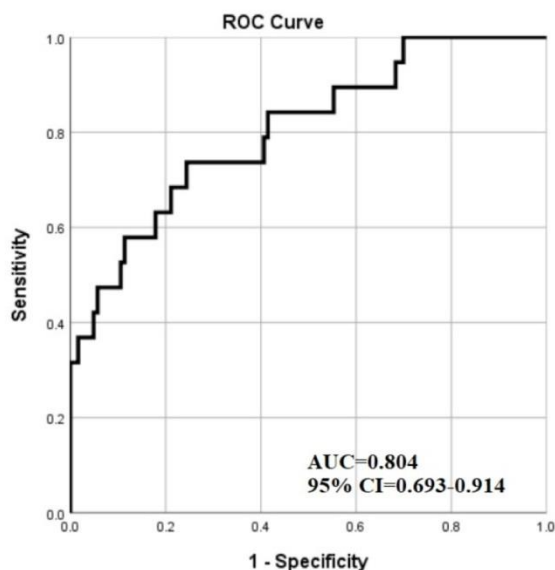
Figure-4. ROC curve of total CQS to predict intensive care necessity. The threshold value of total CQS in distinguishing patients who needed to be transferred to the ICU in the follow-up period was 13.51 (AUC=0.804, 95% CI=0.693-0.914). This cutoff value had 85% sensitivity and 60% specificity. CQS, Computer-aided quantitative score, AUC, Area under the curve; CI, Confidence interval; ROC, Receiver operator characteristics.

DISCUSSION

This study showed higher total CQSs in ICU patients than non-ICU patients and a positive correlation between total VSS and CQS. Furthermore, the study found that underlying fibrosis, the presence of air bubbles, and the co-occurrence of central and peripheral lung area

involvement were the CT findings that were more frequently observed in patients who required intensive care during the follow-up period.

Previous studies have demonstrated the common CT pattern of COVID-19 pneumonia during its early stages and the temporal changes in these findings (8-14). In complete agreement with these reports, pure GGO was the most common CT feature seen in our patients, followed by GGO with consolidation, crazy-paving pattern, pure consolidation, reverse halo sign, and halo sign. Classifying these lesions according to their density and morphology can give a clue about the course of the disease; however, our results here show that this type of evaluation is not of significant value in predicting patients who will require intensive care during the follow-up period. Among findings defined as accompanying CT features of COVID-19 pneumonia such as air-bronchogram, subpleural line, vascular enlargement, air-bubble sign, and bronchiectasis, only the air-bubble sign was observed at significantly higher rates in the ICU-requiring patients. Underlying fibrosis was another distinguishing factor that was significantly higher in the ICU group. As for the results regarding distribution, ICU patients had lesions showing both central and peripheral distribution, whereas most of the lesions in the non-ICU patients were peripherally distributed. Also, lesions in the non-ICU patients showed a predilection to the lower lung zones. These findings support the importance of quantifying data based not only on morphological characteristics but also on distribution patterns that reflect the extent of involvement. From this point of view, recent studies have explored the value of several visual semi-quantitative and software-based quantitative scoring systems in assessing disease severity.

Here we used the scoring system defined by Chung et al. to obtain the visual semi-quantitative scores ranging between 0 (no involvement) to 20 (maximum involvement) (7). We found that the total VSSs of ICU patients were significantly higher than those of non-ICU patients. In their study that included 21 patients, Chung et al. reported that the patient with the highest lung severity score resulted in intensive care unit admission. Similarly, Li et al., using the same method, reported significantly higher total severity scores in severe/critical type patients, where they used a cut-off value of 7.5 that yielded an 82.6% sensitivity and 100% specificity

(15). Pan et al. used a similar semi-quantitative scoring system ranging from 0 to 25 to determine the change in chest CT findings associated with COVID-19 pneumonia from initial diagnosis until patient recovery (4). They showed that most of the patients who recovered from COVID-19 pneumonia had the greatest severity of lung involvement on approximately the 10th day following the onset of symptoms. Yang et al. subjectively evaluated 20 regions of the lung using a scoring system ranging from 0 to 40, attributing scores of 0 (no involvement), 1 (<50% involvement), and 2 (>50% involvement) to each region (16). They found that the scores differed significantly between the mild and severe patient groups. Their most optimal computed tomography severity score cut-off value to expedite the triage of patients needing hospital admission demonstrated an 83.3% sensitivity and 94% specificity. Yuan et al. designed a scoring system for mortality prediction based on the extent of involvement and lesion morphologies (17). The four-point lung parenchyma distribution scale was multiplied by the three-point radiologic scale for each of the six lung zones. Products from all zones were summed up to obtain a cumulative score that ranges from 0 to 72. They found an optimal cut-off value of 24.5 that showed a mortality prediction sensitivity of 85.6% and a specificity of 84.5%. Wasilewski et al. compared the currently available scoring systems in their review article and described another method in which a score between 0 to 20 is assigned to each lung lobe depending on the ratio of involvement, which we also preferred here as the optimal scoring system for diagnosticians to follow (5). They also suggested that a modification of this system that includes additional qualitative features of lung involvement such as GGO, crazy-paving pattern, and consolidations will be useful in evaluating the stage of COVID-19 and the severity of the disease.

Computer-aided quantitative CT assessment is a valuable method for distinguishing confirmed COVID-19 patients from non-COVID-19 patients and assessing disease severity in COVID-19 patients, thanks to its ability to provide an objective measure of the disease extent. Zhang et al. described an artificial intelligence (AI) system that utilizes two models, a lung-lesion segmentation model, and a diagnosis analysis model, to diagnose COVID-19 pneumonia and to distinguish it from other common pneumonia types as well as from healthy controls, using an extensive CT database of 3777 patients (18). They found a good correlation between lesion features on the CT scans and the clinical/biochemical markers of disease severity. They made their AI system publicly available. In addition, many similar studies have used other available software systems, including Thoracic VCAR v13.1 (GE Healthcare), uAI Discover-2019nCoV (Shanghai United Imaging Intelligence Healthcare), 3D Slicer software (version 4.10.2, https://www.slicer. org/), Horos software Version 3.3.3 (https://horosproject.org/) (19-22). Caruso et al. evaluated 190 patients to distinguish between COVID-19 and non-COVID-19 patients using quantitative chest CT (19). They showed the ability of CT quantification of ground-glass opacities and fibrotic alterations to identify COVID-19 patients with moderate accuracy. Unlike this study, our study included patients with COVID-19 pneumonia confirmed by RT-PCR and visual CT evaluation. We performed a purely lesion-focused quantitative analysis and compared this approach with the visual semi-quantitative method. We also evaluated its value in predicting disease severity. We found significant positive correlations between CQSs and VSSs of the total lung and between the scores obtained from each lobe. Cheng et al. also showed good correlations between the conventional semi-quantitative CT score and total lesion-based as well as GGO-based and consolidation-based quantitative assessment results (20). In their study aiming to assess disease severity on admission, they evaluated consolidation and ground-glass opacities separately and showed a higher percentage of consolidation and total infection in ICU patients than non-ICU patients. Yin et al. compared quantitative CT parameters with semi-quantitative visual scores and suggested that quantitative CT parameters are more accurate than the semi-quantitative visual scores in determining COVID-19 severity (21). Ufuk et al. found a significant correlation between the disease severity and quantitative CT scores and found a cut-off value to distinguish between limited (mild, common) and extensive (severe, critical) disease, with 84.6% sensitivity and 77.2% specificity (22). In our study, CQSs were significantly higher in ICU patients than non-ICU patients. The cut-off value of CQSs in predicting patients requiring intensive care in the follow-up period had similar sensitivity (85%) but lower specificity (60%). This level of

variability between different software in quantitative measurements is expected and acceptable. Grassi et al. compared different commercial software for the quantification of COVID-19 pneumonia lesions and reported that providing a fast and semi-automated segmentation of lesions and visualization of infiltrated lung areas such as consolidations, ground-glass opacities, emphysematous areas, and crazy-paving are the advantages of Thoracic VCAR that make it one of the easiest and most efficient tools for automated quantitative measurements in COVID-19 patients (6). Gravity-dependent atelectasis and resultant opacities distributed in the posterior lung areas mistakenly marked as pneumonia sites by the software tools may be another source of poor specificity. Obtaining images in the prone position, especially in patients with respiratory and cardiac problems, may yield better results in the quantitative and semi-quantitative assessment of COVID-19 pneumonia (23).

This study had some limitations. First, this was a retrospective study, which could lead to observer bias and statistical bias. Second, the number of patients in the intensive care arm was limited. Future prospective studies with a larger cohort are needed. Finally, clinical data were limited to whether a patient required intensive care during the follow-up period. Further studies including additional clinical parameters will provide more accurate results in severity assessment.

CONCLUSION

In conclusion, computer-assisted quantitative assessment and visual assessment seem to be useful approaches to assist radiologists in the severity assessment of COVID-19 pneumonia.

Conflict of interest: The authors declare that there is not any conflict of interest regarding the publication of this manuscript.

References

1. Diao K, Han P, Pang T, Li Y, Yang Z. HRCT imaging features in representative imported cases of 2019 novel coronavirus pneumonia. Precis Clin Med. 2020;3(1):9-13.

2. Salehi S, Abedi A, Balakrishnan S, Gholamrezanezhad A. Coronavirus Disease 2019 (COVID-19): A Systematic Review of Imaging Findings in 919 Patients. AJR Am J Roentgenol. 2020;215(1):87-93.

3. Ding X, Xu J, Zhou J, Long Q. Chest CT findings of COVID-19 pneumonia by duration of symptoms. Eur J Radiol.2020;127:109009.

4. Pan F, Ye T, Sun P, et al. Time Course of Lung Changes at Chest CT during Recovery from Coronavirus Disease 2019 (COVID-19). Radiology. 2020;295(3):715-21.

5. Wasilewski PG, Mruk B, Mazur S, Półtorak-Szymczak G, Sklinda K, Walecki J. COVID-19 severity scoring systems in radiological imaging - a review. Pol J Radiol. 2020;85:e361-e368.

6. Grassi R, Cappabianca S, Urraro F, et al. Chest CT Computerized Aided Quantification of PNEUMONIA Lesions in COVID-19 Infection: A Comparison among Three Commercial Software. Int J Environ Res Public Health. 2020;17(18):6914.

7. Chung M, Bernheim A, Mei X, et al. CT Imaging Features of 2019 Novel Coronavirus (2019-nCoV). Radiology. 2020;295(1):202-7.

8. Fang Y, Zhang H, Xie J, et al. Sensitivity of Chest CT for COVID-19: Comparison to RT-PCR. Radiology. 2020;296(2):E115-E117.

9. Yoon SH, Lee KH, Kim JY, et al. Chest Radiographic and CT Findings of the 2019 Novel Coronavirus Disease (COVID-19): Analysis of Nine Patients Treated in Korea. Korean J Radiol. 2020;21(4):494–500.

10. Wu J, Wu X, Zeng W, et al. Chest CT Findings in Patients With Coronavirus Disease 2019 and Its Relationship With Clinical Features. Invest Radiol. 2020; 55(5):257–61.

11. Çinkooğlu A, Hepdurgun C, Bayraktaroğlu S, Ceylan N, Savaş R. CT imaging features of COVID-19 pneumonia: initial experience from Turkey. Diagn Interv Radiol. 2020;26(4):308-14.

12. Song F, Shi N, Shan F, et al. Emerging 2019 Novel Coronavirus (2019-nCoV) Pneumonia. Radiology. 2020;297(3):E346.

13. Li M, Lei P, Zeng B, et al. Coronavirus Disease (COVID-19): Spectrum of CT Findings and Temporal Progression of the Disease. Acad Radiol. 2020;27(5):603-8.

14. Ye Z, Zhang Y, Wang Y, Huang Z, Song B. Chest CT manifestations of new coronavirus disease 2019 (COVID-19): a pictorial review. Eur Radiol. 2020;30(8):4381-9.

15. Li K, Fang Y, Li W, et al. CT image visual quantitative evaluation and clinical classification of coronavirus disease (COVID-19). Eur Radiol. 2020;30(8):4407-16.

16. Yang R, Li X, Liu H, et al. Chest CT Severity Score: An Imaging Tool for Assessing Severe COVID-19. Radiol Cardiothorac Imaging. 2020;2(2):e200047.

17. Yuan M, Yin W, Tao Z, Tan W, Hu Y. Association of radiologic findings with mortality of patients infected with 2019 novel coronavirus in Wuhan, China. PLoS One. 2020;15(3):e0230548.

18. Zhang K, Liu X, Shen J, et al. Clinically Applicable AI System for Accurate Diagnosis, Quantitative Measurements, and Prognosis of COVID-19 Pneumonia Using Computed Tomography. Cell. 2020;181(6):1423-33.

19. Caruso D, Polici M, Zerunian M, et al. Quantitative Chest CT analysis in discriminating COVID-19 from non-COVID-19 patients. Radiol Med. 2021;126(2):243-9.

20. Cheng Z, Qin L, Cao Q, et al. Quantitative computed tomography of the coronavirus disease 2019 (COVID-19) pneumonia. Radiol Infect Dis. 2020;7(2):55-61.

21. Yin X, Min X, Nan Y, et al. Assessment of the Severity of Coronavirus Disease: Quantitative Computed Tomography Parameters versus Semiquantitative Visual Score. Korean J Radiol. 2020;21(8):998-1006.

22. Ufuk F, Demirci M, Uğurlu E, Çetin N, Yiğit N, Sarı T. Evaluation of disease severity with quantitative chest CT in COVID-19 patients. Diagn Interv Radiol. 2021;27(2):164-171.

23. Gürün E. , Akdulum İ. , Akyüz M. Revealing the dilemma in COVID-19 pneumonia: use of the prone thorax CT imaging in differentiation of opacificities due to dependant zone and pneumonic consolidation. Anatolian Curr Med J. 2021; 3(1): 78-80.